JOURNAL OF Materials CHEMISTRY

Differential etch rates in z-cut $LiNbO_3$ for variable HF/HNO_3 concentrations

Collin L. Sones, Sakellaris Mailis, William S. Brocklesby, Robert W. Eason* and John R. Owen

Optoelectronics Research Centre and Department of Chemistry, University of Southampton, Southampton, UK SO17 1BJ. E-mail: rwe@orc.soton.ac.uk

Received 16th July 2001, Accepted 15th November 2001
First published as an Advance Article on the web 29th November 2001

We report the experimental measurements for etch rates of the +z and −z faces of single crystal lithium niobate immersed in HF and HNO_3 acid mixtures of varying ratios. We find that pure HF produces an etch rate that is a factor of 2 higher than the rate obtained for the more frequently used mixture of HF/HNO_3 in a 1 : 2 ratio. We further observe that the quality of etching is improved for either pure HF or HF/HNO_3 in a 1 : 4 ratio, again by comparison with use of a 1 : 2 ratio. These results lead to a discussion of the etch chemistry involved, and an explanation for the observed high degree of differential etching between the +z and −z crystal faces.

1. Introduction

Ferroelectric hosts such as lithium niobate, $LiNbO_3$, and lithium tantalate, $LiTaO_3$, have recently been investigated for their use in microstructured optical and nonlinear optical applications. Both of these hosts possess large values of nonlinear optical, piezoelectric, electro-optical, pyroelectric and acousto-optical coefficients, and attention is currently being given to their use in micro-electro-mechanical (MEMS) devices, and optical MEMS.[1,2]

Of prime importance for MEMS is the ability to fabricate structures with dimensions in the μm to nm range, and recent work has been directed at techniques that can achieve this.[3–5] In its normal single-crystal single-domain state however, there are few successful methods for such precision machining. This contrasts with silicon for example, where anisotropic etching is routinely used to fabricate precision alignment structures such as V-grooves. If domain inversion is performed in z-cut $LiNbO_3$ using photolithographic patterning followed by electric field poling, the technique of differential etching can subsequently be used to produce deep, high aspect ratio structures, with side-walls that can be extremely smooth.[3] The anti-parallel domains produced experience etch rates that are very different. At room temperature, in a 1 : 2 mixture of HF and HNO_3 acids, the −z face experiences etch rates of $\sim 1\ \mu m\ h^{-1}$, whereas the +z face remains unetched in all the experiments we have conducted so far. Even at elevated temperatures of up to 95 °C, where the −z etch rate increases to $\sim 30\ \mu m\ h^{-1}$, the +z face appears not to etch at all, apart from at isolated sites where defects or dislocations may occur.

In this paper we further examine the behaviour of the etch process for domain engineered samples in specific ratios of the HF/HNO_3 mixtures. The earliest reference we have found to this particular etch is listed in the definitive text on $LiNbO_3$ [6] as that of ref. 7 and the 1 : 2 ratio for HF/HNO_3 has since been widely adopted as the mixture of choice for revealing domain inverted regions. More recently etching studies have been undertaken on both periodic structures,[8] and microdomains,[9] using respectively the 1 : 2 ratio and HF alone, but neither of these works reports any systematics concerning etch rates as a function of etch chemistry, or the mechanism behind *differential* etching. To this end, we have performed a parametric study of etch rates and etch quality as a function of the specific ratio of HF/HNO_3, both to ascertain whether this 1 : 2 mixture is in fact optimum for achieving the largest differential etch rates, and also to investigate whether it affects a second differential etch behaviour that we have recently observed in the etching of newly poled *versus* virgin material.

2. Materials and etching methods

All the $LiNbO_3$ samples used were from Crystal Technology, USA, and were supplied as 76 mm diameter, 500 μm thick optically polished z-cut wafers. After dicing and cleaning, samples were spin coated with Shipley 1813 photoresist to a thickness of ∼1 μm, photolithographically patterned and subsequently developed to produce a 6 mm × 20 mm rectangular region in the middle of a larger sample. The patterned regions of the single crystal samples were engineered to produce anti-parallel domains, by applying an electric field exceeding the intrinsic coercive field of $22\ kV\ mm^{-1}$ for the crystal. This technique (referred to as poling) is a standard method for achieving domain inversion in ferroelectrics such as $LiNbO_3$.[10]

Following the electric field poling of this rectangular area as detailed in ref. 3 the sample was then cut into four separate samples each of which had a 6 mm × 5 mm domain inverted region. This procedure of selecting regions from one single larger sample was important to ensure as much uniformity as possible in both the source material, and the process technology associated with photolithography and poling. Each sample was then immersed in different mixtures of HF and HNO_3 acids, and subjected to stirred hot etching at a temperature of 60 °C for 15 hours. The HF was a 48% solution, while the nitric acid was a 78% solution in H_2O. All the chemicals used were supplied by Fisher Scientifics, UK, and were of electronic grade. The samples were held in a specially designed PTFE holder, which was kept immersed within a PTFE beaker containing the etchant. An integral hotplate with a magnetic stirrer regulated the temperature and also ensured uniform etching of the sample faces by continuously stirring the etchant.

The ratios of the HF/HNO_3 acids were chosen to span the most usually quoted value of 1 : 2 for HF/HNO_3. As stated earlier, it is not apparent why this specific ratio has been used so often to date, and so ratios of 1 : 0 (pure HF) 2 : 1, 1 : 1, 1 : 2 and 1 : 4 were chosen to include this 1 : 2 ratio for comparison. After hot etching, all four samples were characterised using a Tencor Alphastep-200 surface profiler for measuring etch

This journal is © The Royal Society of Chemistry 2002

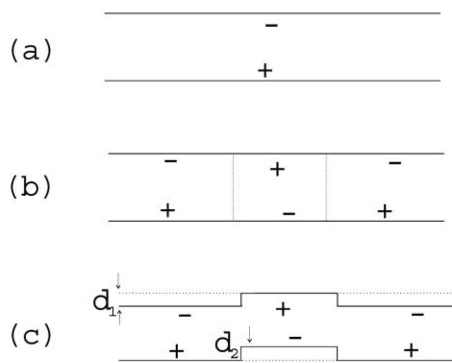

Fig. 1 Schematic showing +z and −z crystal faces, before poling (a), after spatially selective poling (b), and after etching (c).

depth, and a JEOL-6400 scanning electron microscope for examining the overall surface micro-topography.

3. Results and discussion

Fig. 1 shows a schematic of the poling and etching geometry that was common to all four samples. The domain inverted region enables a dual study of the dependence of the differential etch rate *versus* etch concentration. As reported earlier, there is an extremely large difference between the etch rates for +z and −z crystal faces. After even prolonged etching for a total of 600 h, the +z face shows no signs of etching, whereas the −z face etches at an average rate of $\sim 0.8\ \mu m\ h^{-1}$ at room temperature. For newly poled regions however, it is also possible to compare the rate of etch for a virgin −z face, and a newly poled −z face. From earlier published works on the polarisation hysteresis, and reduction of the coercive field for back-poling compared to forward poling,[11–13] there is good reason to suppose that these two rates may also be different. As reported in ref. 13 for example, an internal field is known to exist within $LiNbO_3$, and following electric field poling a newly inverted domain region will have a different value of resultant coercive field. This internal field may then influence the rate of etching, which would be observable *via* different experimental values for etch rate for virgin and newly poled regions.

Fig. 1(c) shows the schematic of measurements for the two different −z faces. Starting from a virgin sample, domain inversion in the central region produces on one face an island of +z in a background of −z, while the other face has a complementary −z island in a background of +z. The depth of the etched material in the first case we have labelled as d_1 whereas the complementary depth on the opposite face is labelled as d_2. Any differential etch rate between different −z faces will result in an effective 'contrast ratio', c, which we define as a

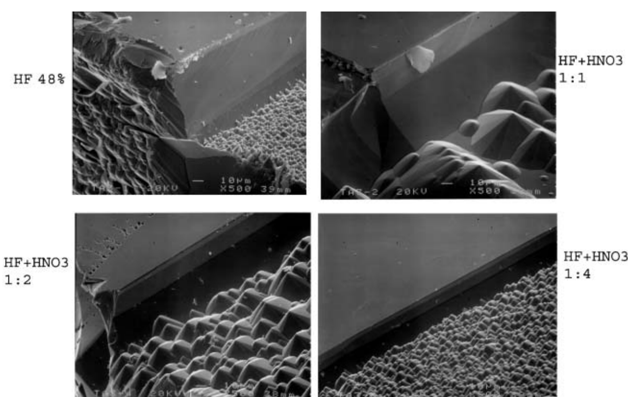

Fig. 2 Scanning electron micrographs showing +z unetched face and etched −z face for four samples of identically poled and processed material. Note the difference in both step height at the edge, and morphology of etched −z surface.

normalised quantity *via* eqn. (1):

$$c = (d_1 - d_2)/(d_1 + d_2) \quad (1)$$

Thus there are two possible differential etch rates involved in this etching study. The first is between the +z and −z faces, while the second refers to the possible differences between a virgin −z face and a newly poled −z face, which might therefore be associated with the presence of this intrinsic internal field.[13]

Fig. 2 shows four SEM micrographs of the structures etched in 1 : 0, 1 : 1, 1 : 2 and 1 : 4 HF/HNO_3 etch mixtures, all stirred for 15 hours at 60 °C. Each micrograph shows a wall feature that separates regions of +z face unetched material, from the −z face which etches normally, exposing structured regions of threefold symmetry which appear as peaks. The side faces of these peaks (which are neither +z nor −z faces) etch at a rate that is different to the −z rate, and therefore some degree of surface roughness, once established, is maintained throughout the etching process. What is immediately apparent is that the widely used 1 : 2 etch ratio is optimum neither in the etch depths achieved, nor in the smoothness obtained for the −z etched surface. For optimum depth and also smoothness, the pure (48%) HF solution is best at the temperature used of 60 °C. Fig. 3 shows plan views of the same etched regions, making the comparison of etch smoothness even more apparent. Such nonuniformity in etching is always present in our experience for congruent $LiNbO_3$. The greatly improved degree of smoothness associated with both pure HF and 1 : 4 HF/HNO_3 etches is of great potential benefit when realising deep 3-D structuring.

Fig. 4 quantifies this etch depth as measured by the alpha-step. For each data point, an average of ten depth measurements was

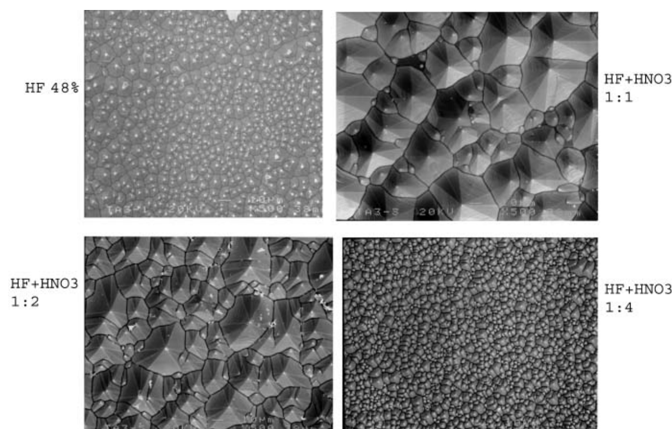

Fig. 3 Plan view of samples in Fig. 2, illustrating differences in morphology of the etched −z surfaces.

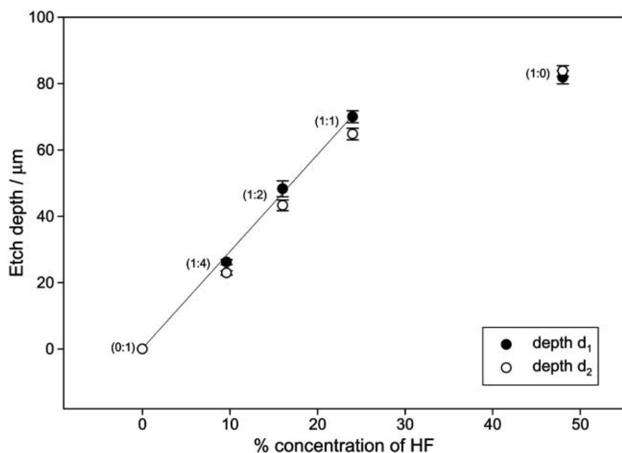

Fig. 4 Measured etch depth for identical samples etched in mixtures of HF/HNO_3 acids. The depth corresponds to etching for 15 hours at a temperature of 60 °C. The straight line is a best fit to the first four data points, and is referred to later in the text (numbers in brackets are ratios of HF/HNO_3).

taken, to cope with the lack of smoothness associated particularly with the 1 : 1 and 1 : 2 etch mixtures. The error bars for each point represent the standard deviations deduced from each set of ten depth measurements. It is again apparent that the 1 : 2 mixture etches approximately half as fast as the pure HF (no HNO_3) etch, labelled as (1 : 0) in Fig. 4. Pure HNO_3 (no HF), labelled as (0 : 1), as expected produced no observable etching. Two sets of data points are included for depths d_1 and d_2 as described *via* Fig. 1. It is clear that there may well be a secondary differential etch rate, quantified *via* the contrast ratio parameter, *c*, given earlier. Fig. 5 shows this explicitly for the data points of Fig. 4. Although the data points are few, and the error bars are large due to the normalisation process, there does indeed appear to be the suggestion of a second differential etch rate for the newly poled *versus* virgin material. This would have very useful applications in some of the MEMS work we are currently involved in, as precise control of etching rates, and specifically back-etching is highly desirable.

A second study was carried out using 48% HF only, diluted in the ratios of 1 : 0, 2 : 1, 1 : 1, 1 : 2 and 1 : 4, HF/H_2O. Fig. 6 shows the etch depths d_1 and d_2 plotted as a function of the percentage concentration of HF, from which it can be seen that the etch rate increases rapidly at an effective threshold of concentration between ∼20–30%. There is also the suggestion of a possible −z face differential etch rate, but this is far less apparent than for the case of HF/HNO_3 etching.

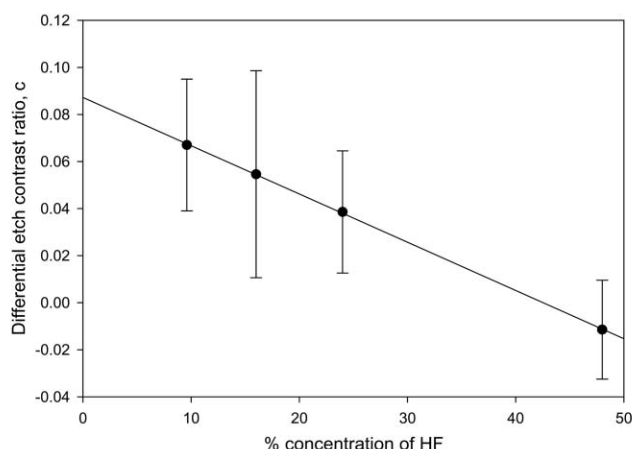

Fig. 5 Differential etch contrast ratio, *c*, plotted as a function of HF concentration for results shown in Fig. 4.

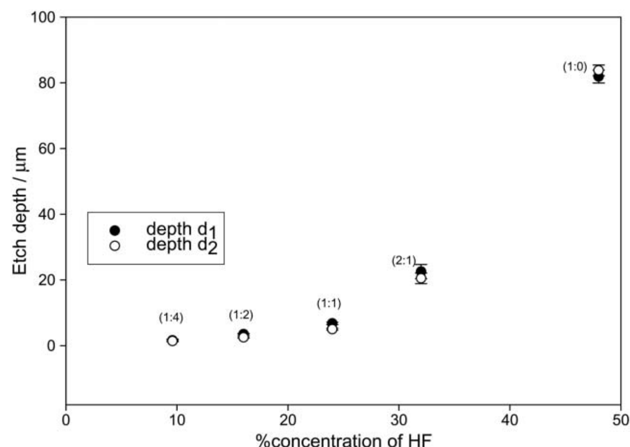

Fig. 6 Measured etch depth for identical samples as a function of HF concentration. The depth corresponds to etching for 15 hours at a temperature of 60 °C.

4. Chemistry of HF/HNO_3 etching and differential etch behaviour

We now need to address the mechanisms behind the HF/HNO_3 etch behaviour, with particular attention to the differential etch behaviour for the +z and −z crystal faces.

The variation of the etch rate with HF concentration in water as shown in Fig. 6 clearly shows that the etch rate increases superlinearly with the HF concentration. In the apparent absence of previous quantitative reports on this etching reaction we refer to a recent study of HF etching of SiO_2, which has a hydroxide-terminated surface similar to what is expected in the present case. Knotter[14] concluded that the etching of SiO_2 in HF solutions was controlled by fluoride substitution of the surface hydroxide. The accelerating effect of a low pH was attributed to the greater extent of surface protonation, leading to hydroxide removal as a precursor to fluoridation by HF_2^-, or H_2F_2 at very low pH.

The highly plausible notion that etching is initiated by surface protonation immediately explains two qualitative observations made in our experiments:

(1) Faster etching on the negative face is due to easier absorption of the positively-charged proton.

(2) The etch rate increases with increasing concentration of acidic protons.

The following discussion will attempt to explain the quantitative observations, namely the superlinear increase with HF concentration in the absence of nitric acid and the almost linear increase with the amount of HF added to concentrated nitric acid.

4.1 HF solutions

The rapid increase as the HF concentration approaches 48% does not correlate with the acid proton concentration computed from the thermodynamic data presented by Knotter.[14] Of many attempted correlations, the one which had the most successful fit and the most plausible physical explanation is shown in Fig. 7, where the rate is plotted against the ratio $c_{HF}/(c_{H_2O} - c_{HF})$ where c_{H_2O} and c_{HF} are the total molar concentrations of water and HF in the mixture. A logarithmic plot is used to show that the etch rate is proportional to this quantity over a range of at least two orders of magnitude. The data point for the 2 : 1 HF/H_2O ratio lies somewhat off the fit that would exist for the other four points. Although there is good reason to exclude this point as it was not obtained at the same time as the first four, and hence there is some possibility of systematic error perhaps in the parameters used for the electric field poling for example, we have chosen to retain this point in the graph.

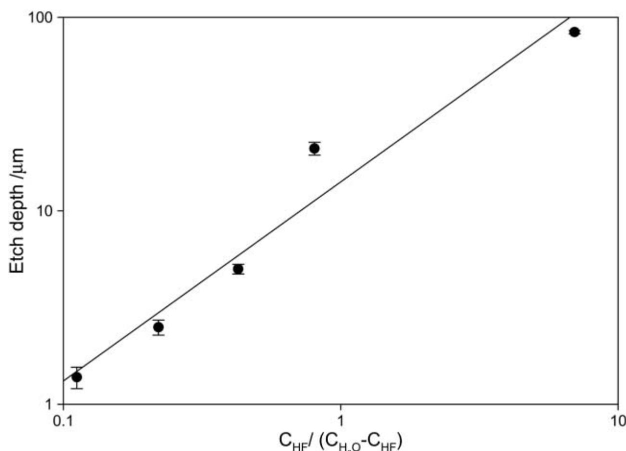

Fig. 7 Log–log plot of etch depth *versus* $c_{HF}/(c_{H_2O} - c_{HF})$ for data shown in Fig. 6. The straight line is a linear regression.

It is suggested here that the inverse correlation with $(c_{H_2O} - c_{HF})$ is due to the reduction of the thermodynamic activity of water at high HF concentrations. It is known that water is complexed by HF to form H_3OF[15] so that only the residual, uncomplexed water would be active in the dehydroxylation equilibrium (2):

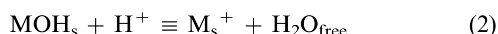

$$MOH_s + H^+ \equiv M_s^+ + H_2O_{free} \quad (2)$$

where MOH_s and M_s represent normal, and dehydroxylated surface groups.

If dehydroxylation only occurs for a small fraction of the surface, due to the weakness of the acid, the concentration of dehydroxylated surface sites can be expressed by eqn. (3):

$$[M_s^+] = K_1[H^+]/[H_2O_{free}] = K_1[H^+]/(c_{H_2O} - c_{HF}) \quad (3)$$

However we should expect a square root dependence of etch rate on c_{HF} from this expression, since the proton concentration itself varies with the square root of c_{HF} according to equilibrium (4):

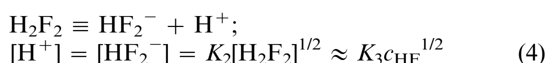

$$H_2F_2 \equiv HF_2^- + H^+; \\ [H^+] = [HF_2^-] = K_2[H_2F_2]^{1/2} \approx K_3 c_{HF}^{1/2} \quad (4)$$

(Our computations from Knotter's data[14] show that H_2F_2 is the majority fluorine-containing species in the system)

The linear dependence of rate on c_{HF} can be explained by assuming that fluoridation of the surface occurs by an electrostatically-enhanced attack of M_s^+ by HF_2^-, eqns. (5) and (6):

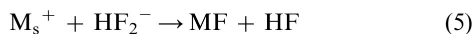

$$M_s^+ + HF_2^- \rightarrow MF + HF \quad (5)$$

$$\text{rate} = k_1[M_s^+][HF_2^-] \\ = k_1K_1[H^+][HF_2^-]/(c_{H_2O} - c_{HF}) \quad \text{(from (3))}$$

$$= k_2 c_{HF}/(c_{H_2O} - c_{HF}) \text{ as required, where } k_2 = k_1K_1K_3^2 \quad (6)$$

4.2 HF/HNO$_3$ solutions

Data for the etch solutions containing HNO_3 show a simpler relation where the etch rate is simply proportional to the HF concentration. The model in this case assumes that nitric acid is probably strong enough to saturate the negatively charged surface with protons, dehydroxylate completely and then cover the M_s^+ surface with nitrate, eqn. (7):

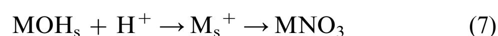

$$MOH_s + H^+ \rightarrow M_s^+ \rightarrow MNO_3 \quad (7)$$

The subsequent reaction is determined by the rate of fluoride substitution at the surface. Here there is no electrostatic enhancement of HF_2^- attack, so that the more abundant H_2F_2 is more effective than HF_2^- in this case, eqn (8) and (9).

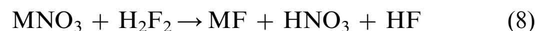

$$MNO_3 + H_2F_2 \rightarrow MF + HNO_3 + HF \quad (8)$$

$$\text{rate} = k_3[H_2F_2] \approx k_4 c_{HF} \quad (9)$$

This proportionality is verified in the data of Fig. 4 which shows a straight line passing close to the origin as expected, since zero HF gave a zero etch rate. One result which did not fit the model is the result at 48% HF, where the model of section 4.1 is more applicable in the absence of nitric acid.

The proposed model also explains the observation that the etch is much faster on the −z crystal face, since a negative surface charge would favour protonation by increasing the value of K_1. Also, the short metal–oxygen bond on the positively charged surface should be more stable, and therefore less reactive, than the long bond on the negative surface

5. Conclusions

A suggested mechanism for the etch rate in aqueous HF involves an initial dehydroxylation of the negatively charged surface by proton attack followed by an electrostatically-enhanced reaction of the subsequent positively-charged surface with HF_2^- anions. The rapid increase in rate near the 48% composition is attributed to the reduction in free water concentration. In aqueous HF/HNO_3 solutions, a linear dependence of etch rate with HF concentration is attributed to attack of a nitrate-covered positive surface by the abundant neutral species H_2F_2. In both cases, an initial protonation is considered essential, and this is much slower on the positively charged face.

Acknowledgements

We are very pleased to acknowledge fruitful discussions with Phil Bartlett and Eleanor Tarbox from the Departments of Chemistry and Optoelectronics Research Centres at the University of Southampton. We also acknowledge research funding support from the Engineering and Physical Sciences Research Councils, under grant numbers GR/N00302 and GR/R47295

References

1 R. W. Eason, I. E. Barry, G. W. Ross, P. G. R. Smith and C. B. E. Gawith, *Proc SPIE*, 2000, **4075**, 124–133.
2 A. J. Boyland, G. W. Ross, S. Mailis, P. G. R. Smith and R. W. Eason, *Electron. Lett.*, 2001, **37**, 585–587.
3 I. E. Barry, G. W. Ross, P. G. R. Smith and R. W. Eason, *Mater. Lett.*, 1998, **37**, 246–254.
4 R. W. Eason, I. E. Barry, G. W. Ross and P. G. R. Smith, *Electron. Lett.*, 1999, **35**, 328–329.
5 I. E. Barry, G. W. Ross, P. G. R. Smith and R. W. Eason, *Appl. Phys. Letts.*, 1999, **74**, 1487–1488.
6 A. M. Prokhorov and Yu. S. Kuz'minov, *Physics and Chemistry of Crystalline Lithium Niobate*, Adam Hilger, Bristol, 1990.
7 K. Nassau, H. J. Levinstein and G. M. Loiacono, *J. Phys. Chem. Solids*, 1966, **27**, 983–988.
8 V. Bermudez, F. Caccavale, C. Sada, F. Segato and E. Dieguez, *J. Cryst. Growth*, 1998, **191**, 589–593.
9 W. L. Holstein, *J. Cryst. Growth*, 1997, **171**, 477–484.
10 M. Yamada, N. Nada, M. Saitoh and K. Watanabe, *Appl. Phys. Lett.*, 1993, **62**, 435–436.
11 S. Chao, W. Davis, D. D. Tuschel, R. Nichols, M. Gupta and H. C. Cheng, *Appl. Phys. Lett.*, 1995, **67**, 1066–1068.
12 P. T. Brown, R. W. Eason, G. W. Ross and A. R. Pogosyan, *Opt. Commun.*, 1999, **163**, 310–316.
13 V. Gopalan and M. C. Gupta, *Ferroelectrics*, 1997, **198**, 49–59.
14 D. M. Knotter, *J.Am.Chem.Soc.*, 2000, **122**, 4345–4351.
15 F. A. Cotton and G. Wilkinson, *Advanced Inorganic Chemistry* Wiley, New York, 5th edn., 1988, p. 104.